Paulina Woźniak
Anna Świątek
Mariusz Pożoga
Łukasz Tomasik

Space Research Centre
Polish Aacademy of Sciences
Warsaw, Poland

Analysis of a new regional ionospheric assimilated **H2PT model** for Europe

European Geosciences Union General Assembly
3-8 May 2020, Vienna, Austria

Table of contents

Basics & data

- introduction
- about H2PT model
  - computational steps
  - data flow
  - parameters
- comparison data

Analysis

- TEC parameter
  - models comparison
    - 5° grid
    - 1° grid
  - time series
- hmF2 parameter
- disturbed conditions – examples

Summary

- conclusions
- contact

Basics & data

GNSS positioning

observed pseudorange

geometric distance between the satellite and the receiver

satellite and receiver clock errors

ionospheric refraction

receiver noise

code measurements: $$P = \rho + \delta\rho + c(\delta t_r - \delta t^s) + \delta T + \delta I + \delta m + \varepsilon$$

phase measurements: $$L = \rho + \delta\rho + c(\delta t_r - \delta t^s) + \lambda N + \delta T - \delta I + \delta m + \varepsilon$$

observed carrier phase

orbital errors

carrier wavelength

carrier phase ambiguity

tropospheric refraction

multipath

GNSS positioning

code measurements: $P = \rho + \delta\rho + c(\delta t_r - \delta t^s) + \delta T + \boldsymbol{\delta I} + \delta m + \varepsilon$

phase measurements: $L = \rho + \delta\rho + c(\delta t_r - \delta t^s) + \lambda N + \delta T - \boldsymbol{\delta I} + \delta m + \varepsilon$

- P – observed pseudorange
- L – observed carrier phase
- ρ – geometric distance between the satellite and the receiver
- $\delta\rho$ – orbital errors
- $c(\delta t_r - \delta t^s)$ – satellite and receiver clock errors
- λ – carrier wavelength
- N – carrier phase ambiguity
- δT – tropospheric refraction
- δI – **ionospheric refraction**
- δm – multipath
- ε – receiver noise

Impact on GNSS observations

Number of e⁻

N_e – number of free electrons in a unit of volume $[e^-/m^3]$ (variable in cross-section)

$$TEC = \int_s^r N_e dl$$

Total Electron Content

TEC – number of free electrons contained in a column with a cross-section of 1 m^2, determined along the path l of signal propagation between the satellite s and the receiver r

Total Electron Content Unit: $1\,[TECU] = 10^{16}\,[e^-/m^2]$

velocity	group	phase
ionospheric refraction	$\delta I_{gr} = +\frac{40{,}3\ \mathrm{TEC}}{f^2}$	$\delta I_{ph} = -\frac{40{,}3\ \mathrm{TEC}}{f^2}$
result	↘	↗

VTEC – vertical TEC

STEC – slant TEC

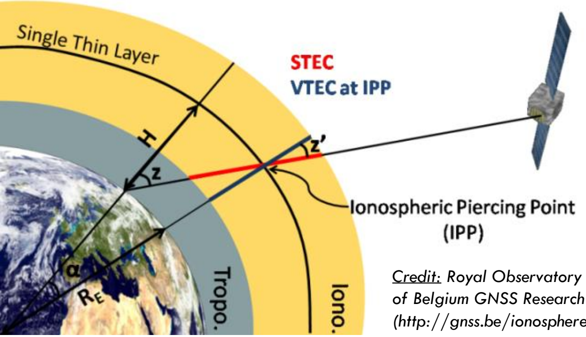

Credit: *Royal Observatory of Belgium GNSS Research Group (http://gnss.be/ionosphere_tutorial.php)*

Ionospheric Pierce Point

IPP – intersection of the ionosphere by the satellite signal in an approximated single layer located at the average height of the maximum electron concentration

Single Layer Model

SLM – in the GNSS data processing, a constant value of the maximum electron concentration height for the entire globe; commonly determined altitude of 450 km

H2PT model

Project

- part of data processing pipe designed for:
  - RINEX *(Receiver Independent Exchange System)* observation file import
  - observation geometry determination
  - searching data based on advanced criteria
- the entire pipeline is supervised by the SCADA (*Supervisory Control and Data Acquisition*) system
- it runs in parallel on computer cluster to reduce computation time

Main tasks

- data gathering:
  - publicly available repositories of GNSS (*Global Navigation Satellite Systems*) permanent reference station networks
    - EPN (*EUREF Permanent Network*)
    - IGS (*International Ground Station*) Network
  - measurement results from ionosondes participating in the DIAS (*European Digital Upper Atmosphere Server*) project
- data processing
- storing results in the efficient database that allows:
  - effective searching
  - quick access to the data

H2PT model – computational steps

1) downloading raw RINEX observation files from network repositories, conversion and storage in the database
2) downloading RINEX navigation files and Almanac data extraction
3) computation of GNSS satellites position (to minimize computational effort) and storage in the database
4) data reviewing, discontinuities and phase shifts elimination (to obtain continuous measurement arcs)
5) selection of arcs for each reference station, for every 12 hour
6) calculation of observation geometry assuming the single-layer ionospheric model
7) computation of phase correction for a given arc using least-square method and storage of VTEC values for the ionospheric pierce point in the database
8) interpolation of VTEC values for individual stations into a 5° x 5° (or 1° x 1°) grid for the succesive 15-minute time periods
9) median determination as the final result for the individual nodes
10) storage of maps in the database (to allow easy access to H2PT solution)

H2PT model – data flow

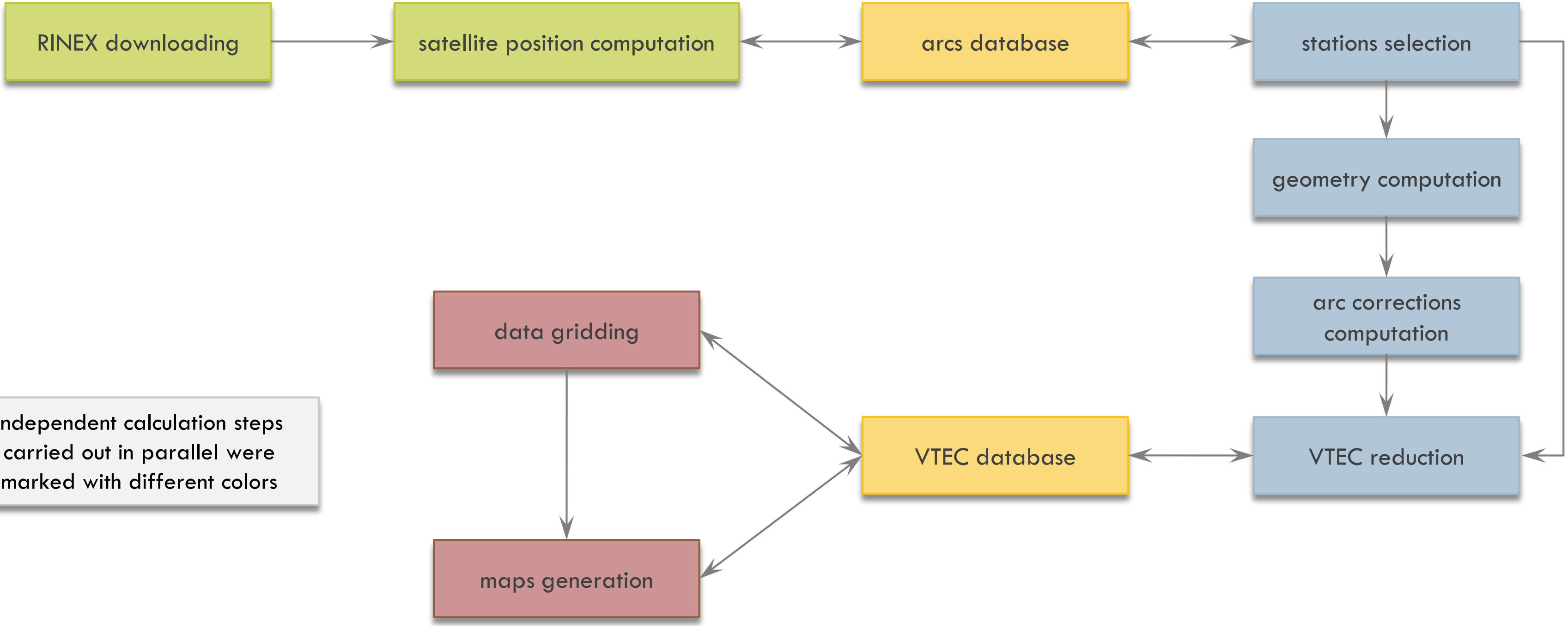

independent calculation steps carried out in parallel were marked with different colors

H2PT model – parameters

Characteristic

- assimilated model
- area: Europe
  - latitude: from 30°N to 70°N
  - longitude: from 10°W to 40°E
- time resolution: 15 min
- spatial resolution:
  - 1° x 1°
  - 5° x 5°
- ionospheric parameters:
  - VTEC (*Vertical Total Electron Content*)
  - hmF2 (*height maximum of the F2 layer*)
- file format: IONEX-like (*IONosphere Map Exchenge*)

Advantages

- regional character
- high spatial resolution enables detailed analysis of occuring ionosphere disturbances
- high temporal resolution allow detection of short-term ionosphere disturbances
- providing data on the hmF2 parameter

Data processing

- information on disturbances: RWC Warszawa – Regional Warning Centre of ISES (*International Space Environment Service*)
- tools: MATLAB

Comparison data

model	IGS (International GNSS Service)	NeQuick-G
institution	GRL/UWM (Geodynamics Research Laboratory, University of Warmia and Mazury)	ICTP (Abdus Salam International Center of Theoretical Physics) University of Graz ESA (European Space Agency)
area	global	global
spatial resolution	2.5° x 5.0°	for the given parameters
time resolution	2 h	
source	CDDIS FTP (Crustal Dynamics Data Information System)	dedicated application

Analysis

TEC parameter

H2PT model, 5° grid; March 10, 2019; (scale: 0 ÷ 20 TECU)

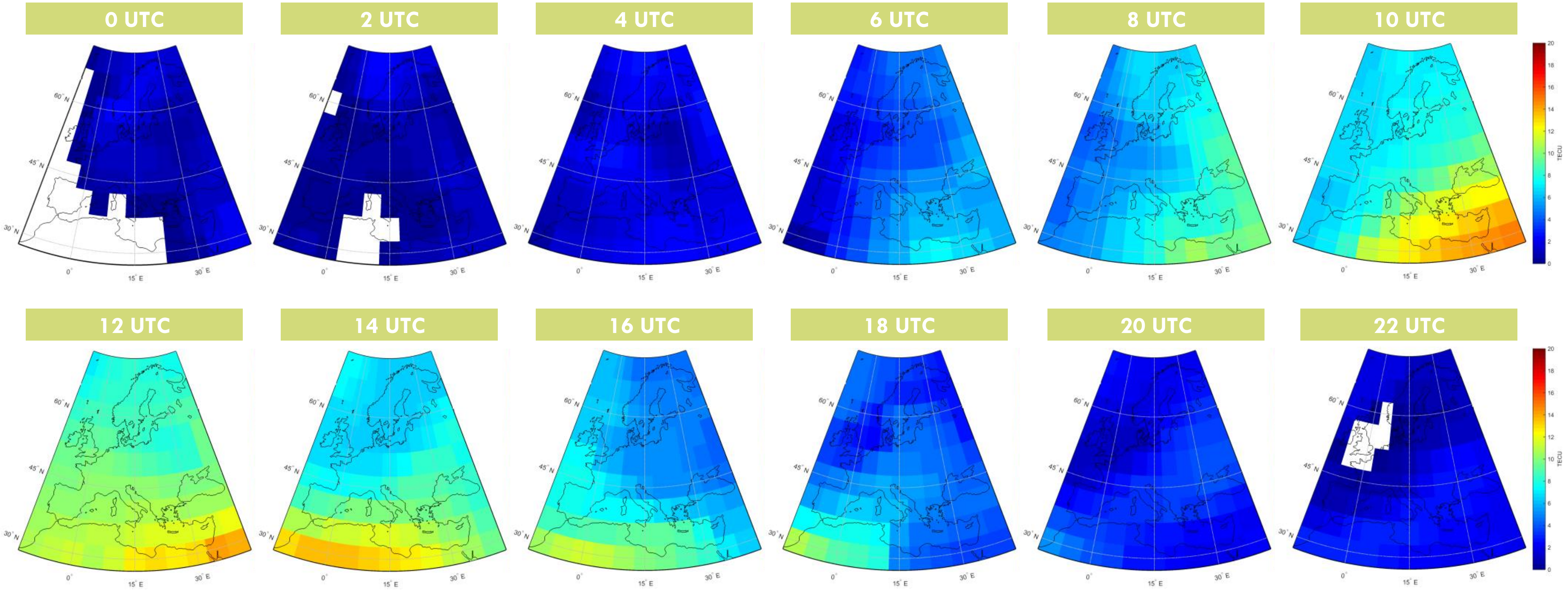

H2PT model, 1° grid; March 10, 2019; (scale: 0 ÷ 20 TECU)

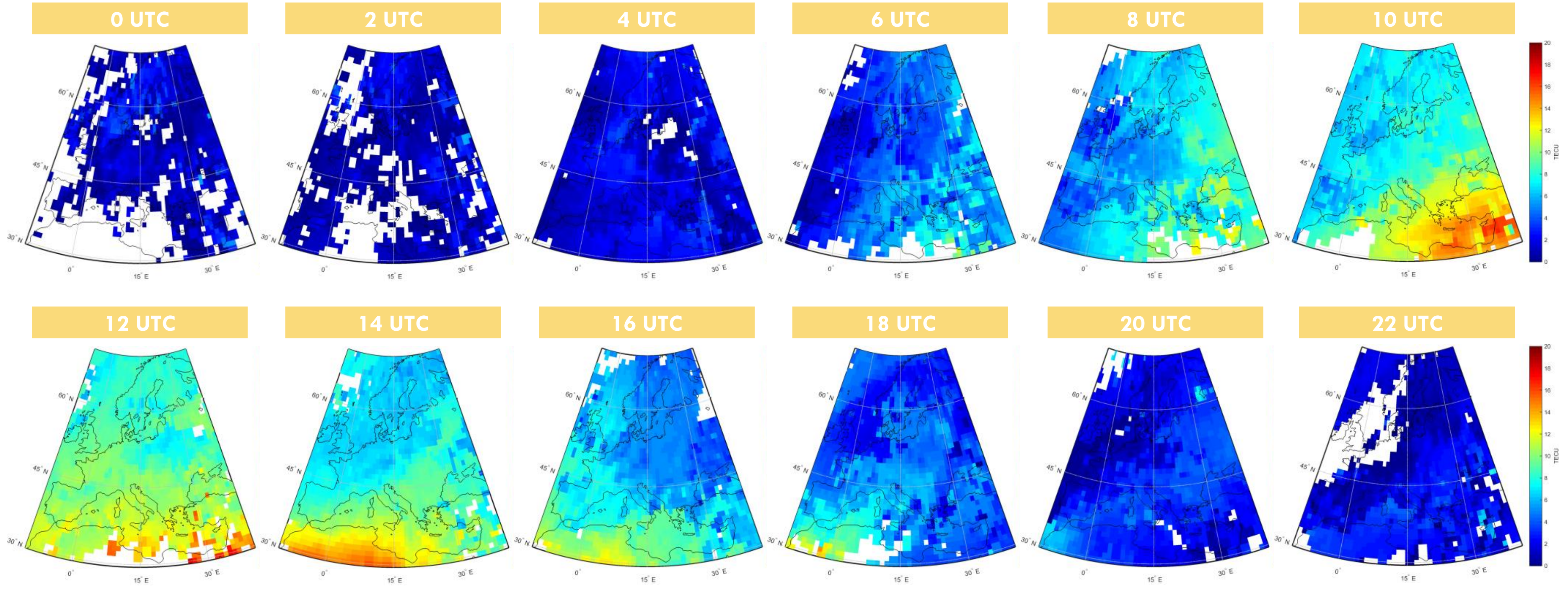

Grid: 5°, H2PT vs IGS, March 10, 2019, 14 UTC

H2PT (scale: 0 ÷ 20 TECU)

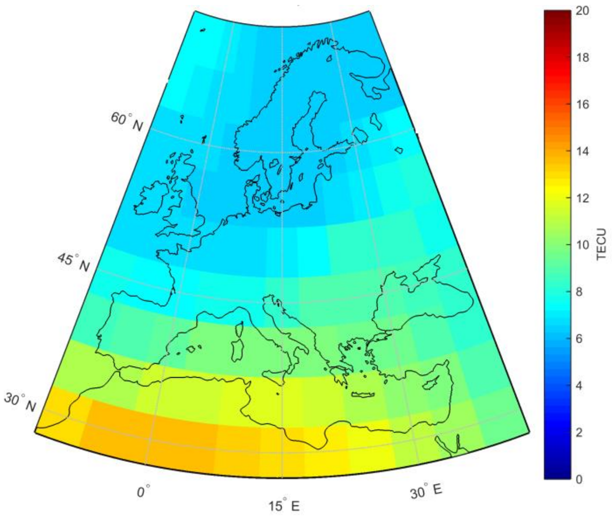

IGS (scale: 0 ÷ 20 TECU)

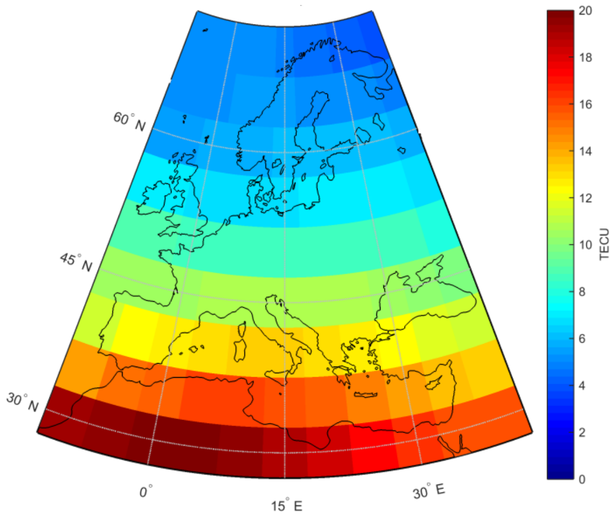

differences (scale: -12 ÷ 8 TECU)

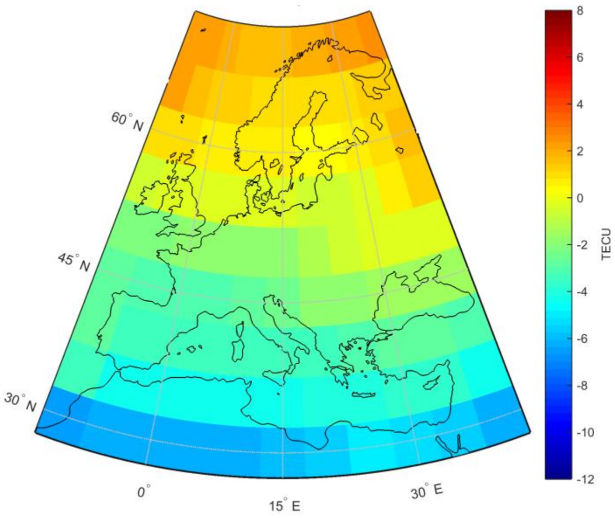

Grid: 5°, H2PT vs NeQuick, March 10, 2019, 14 UTC

H2PT (scale: 0 ÷ 20 TECU)

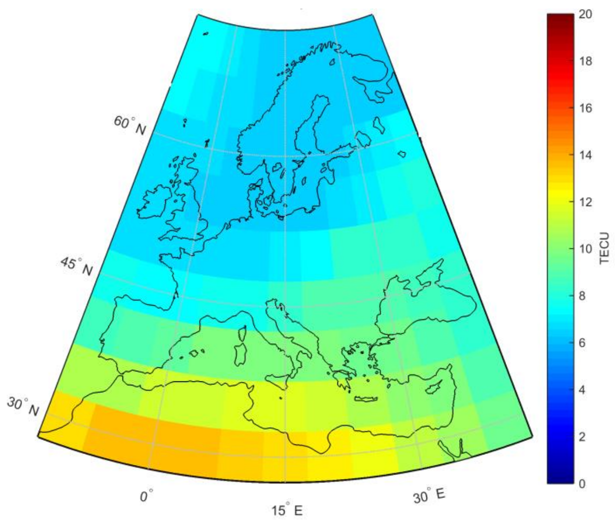

NeQuick-G (scale: 0 ÷ 20 TECU)

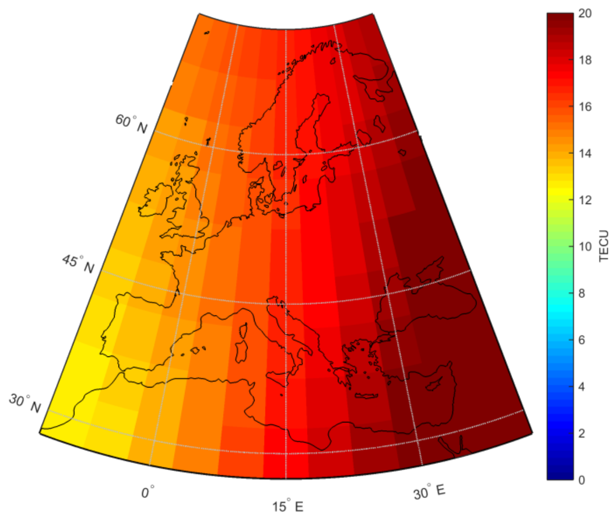

differences (scale: -12 ÷ 8 TECU)

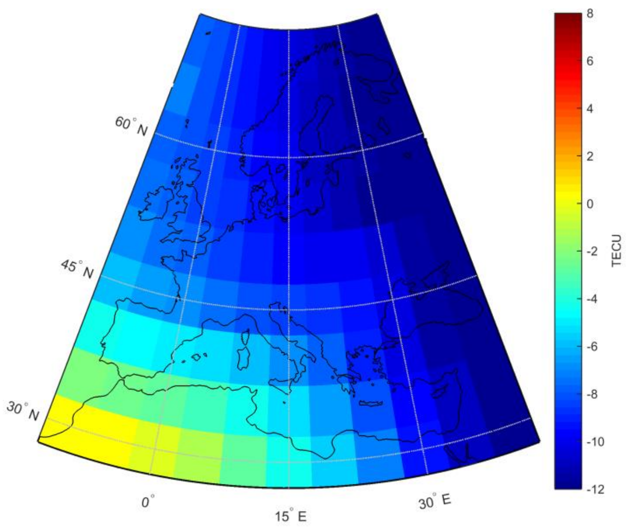

Differences: H2PT – IGS, grid: 5°; March 10, 2019

(scale: -12 ÷ 8 TECU)

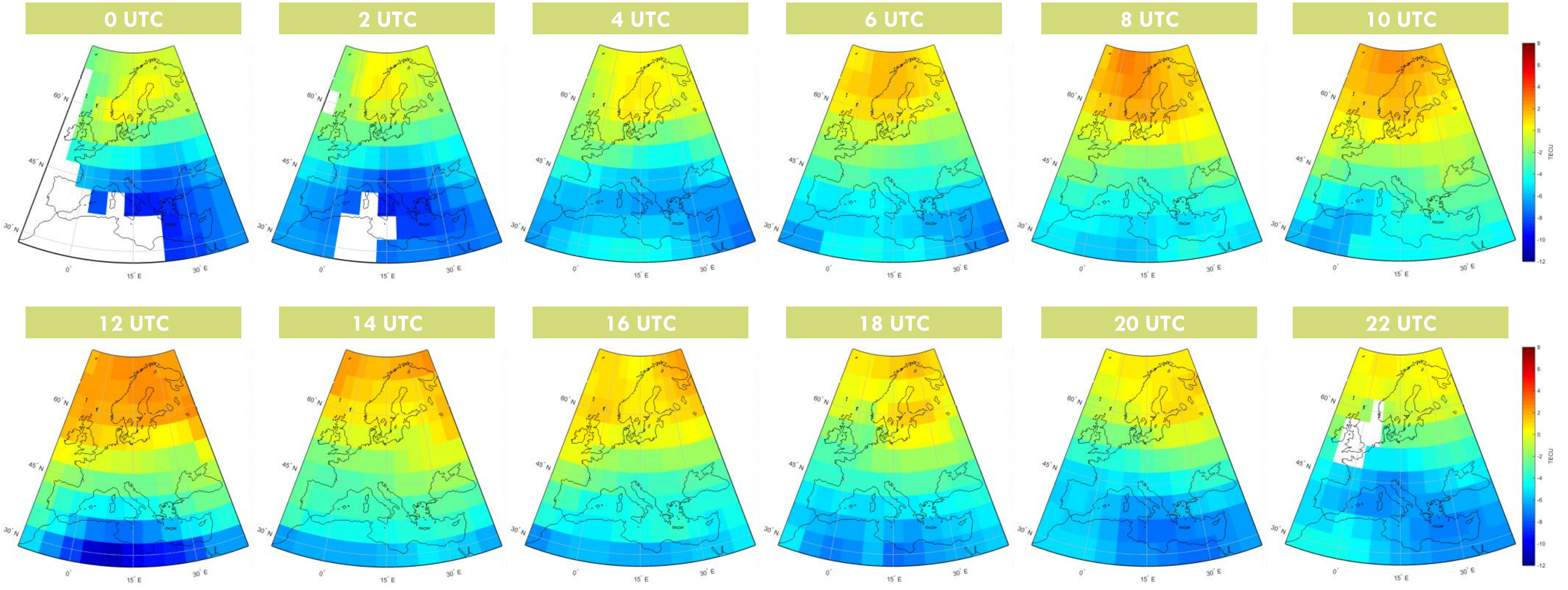

Differences: H2PT – NeQuick, grid: 5°; March 10, 2019

(scale: -12 ÷ 8 TECU)

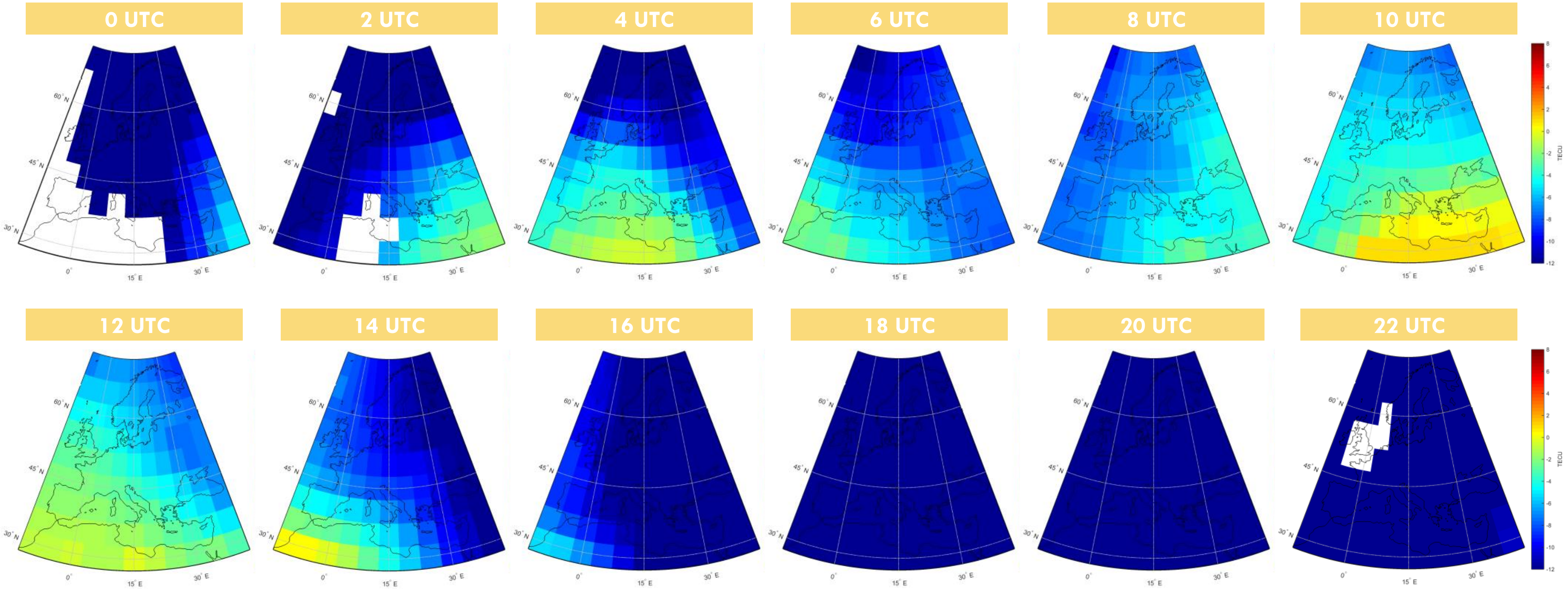

Statistical parameters, grid: 5°, March 10, 2019

2 UTC	min [TECU]	max [TECU]	amplitude [TECU]	mean [TECU]	σ [TECU]	correlation coefficient [-]
H2PT	0,2	2,4	2,2	0,78	0,60	
IGS	1,5	8,9	7,4	4,99	2,71	
NeQuick	3,0	17,6	14,6	11,29	3,99	
$\Delta_{H2PT-IGS}$	-8,9	0,6	9,5	-4,05	3,01	-0,46
$\Delta_{H2PT-NeQuick}$	-17,0	-2,0	15,0	-10,64	3,92	0,26

8 UTC	min [TECU]	max [TECU]	amplitude [TECU]	mean [TECU]	σ [TECU]	correlation coefficient [-]
H2PT	3,8	10,5	6,7	6,57	1,48	
IGS	3,2	14,9	11,7	8,03	3,43	
NeQuick	11,8	14,4	2,6	12,84	0,60	
$\Delta_{H2PT-IGS}$	-5,8	2,7	8,5	-1,45	2,77	0,62
$\Delta_{H2PT-NeQuick}$	-10,0	-2,4	7,6	-6,27	1,48	0,22

14 UTC	min [TECU]	max [TECU]	amplitude [TECU]	mean [TECU]	σ [TECU]	correlation coefficient [-]
H2PT	6,3	13,5	7,2	8,28	2,09	
IGS	3,9	19,8	15,9	9,71	4,50	
NeQuick	12,5	22,3	9,7	16,87	2,23	
$\Delta_{H2PT-IGS}$	-6,4	2,4	8,8	-1,43	2,57	0,96
$\Delta_{H2PT-NeQuick}$	-13,1	0,4	13,5	-8,59	3,14	-0,01

20 UTC	min [TECU]	max [TECU]	amplitude [TECU]	mean [TECU]	σ [TECU]	correlation coefficient [-]
H2PT	1,0	5,1	4,1	2,59	0,89	
IGS	1,3	10,5	9,2	5,58	3,27	
NeQuick	18,8	24,5	5,7	21,40	1,43	
$\Delta_{H2PT-IGS}$	-7,5	1,2	8,7	-3,00	2,94	0,49
$\Delta_{H2PT-NeQuick}$	-22,5	-15,6	6,9	-18,81	1,63	0,06

Grid: 1°, H2PT vs IGS, March 10, 2019, 14 UTC

H2PT (scale: 0 ÷ 20 TECU)

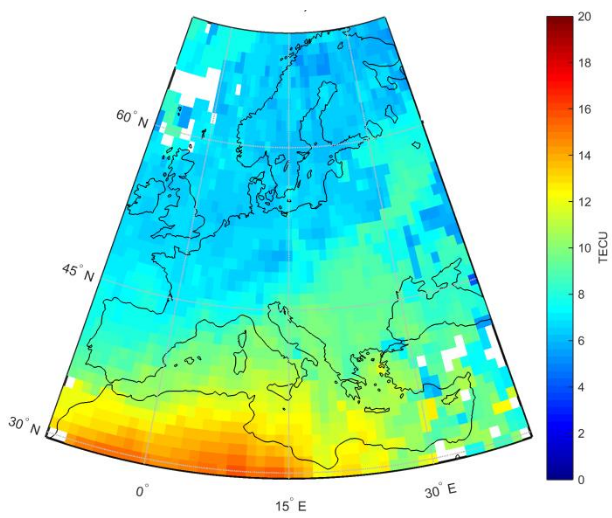

IGS (scale: 0 ÷ 20 TECU)

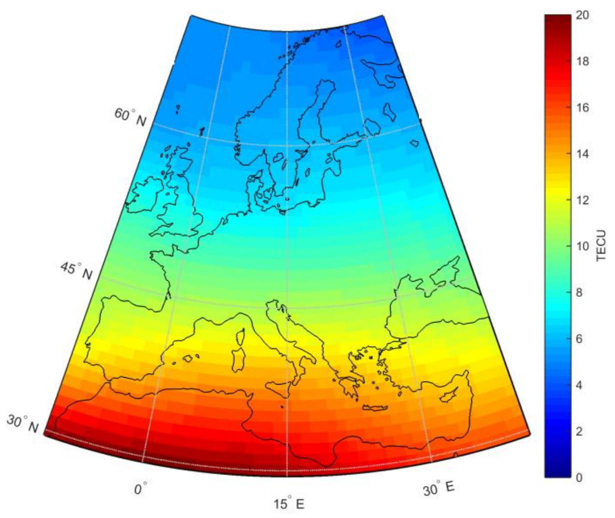

differences (scale: -12 ÷ 8 TECU)

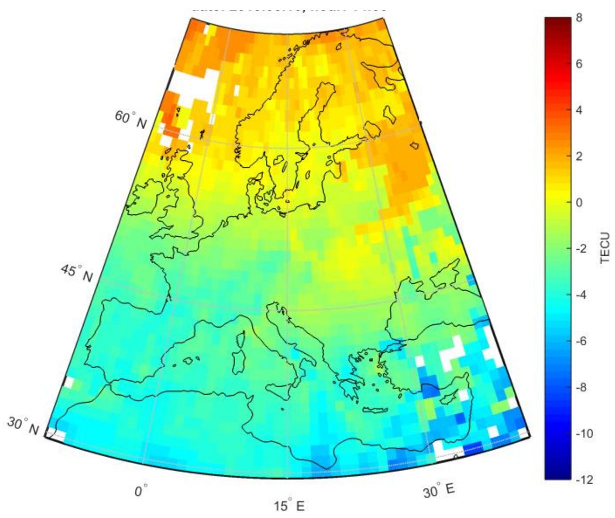

Grid: 1°, H2PT vs NeQuick, March 10, 2019, 14 UTC

H2PT (scale: 0 ÷ 20 TECU)

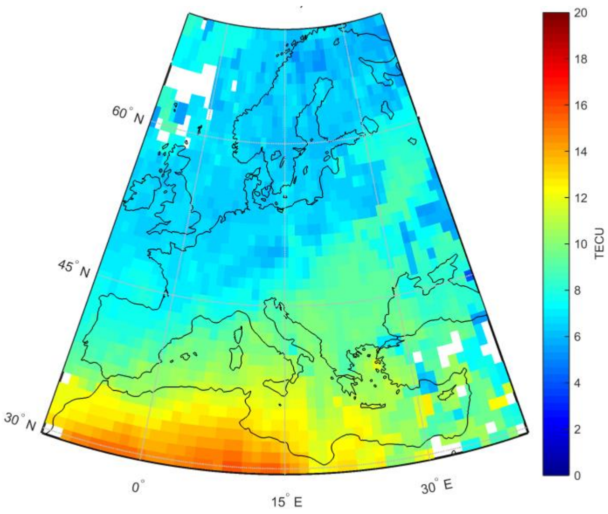

NeQuick-G (scale: 0 ÷ 20 TECU)

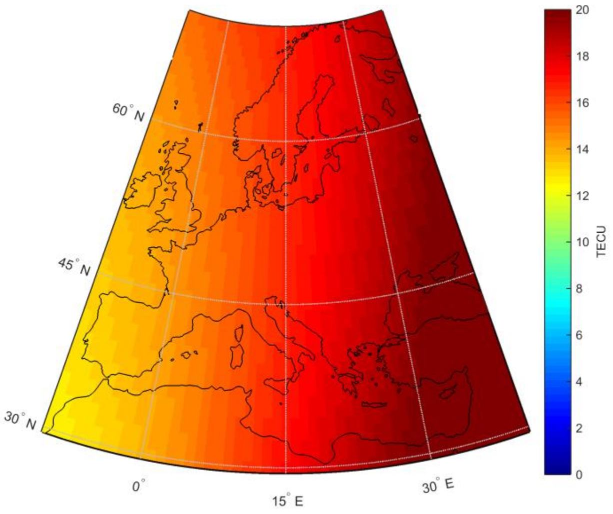

differences (scale: -12 ÷ 8 TECU)

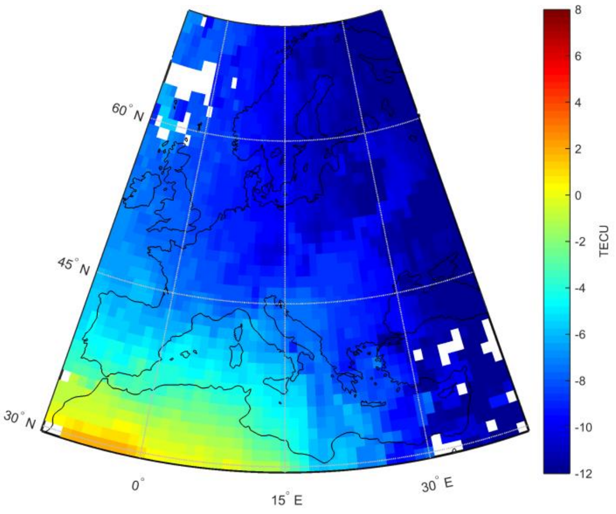

Differences: H2PT – IGS, grid: 1°; March 10, 2019

(scale: -12 ÷ 8 TECU)

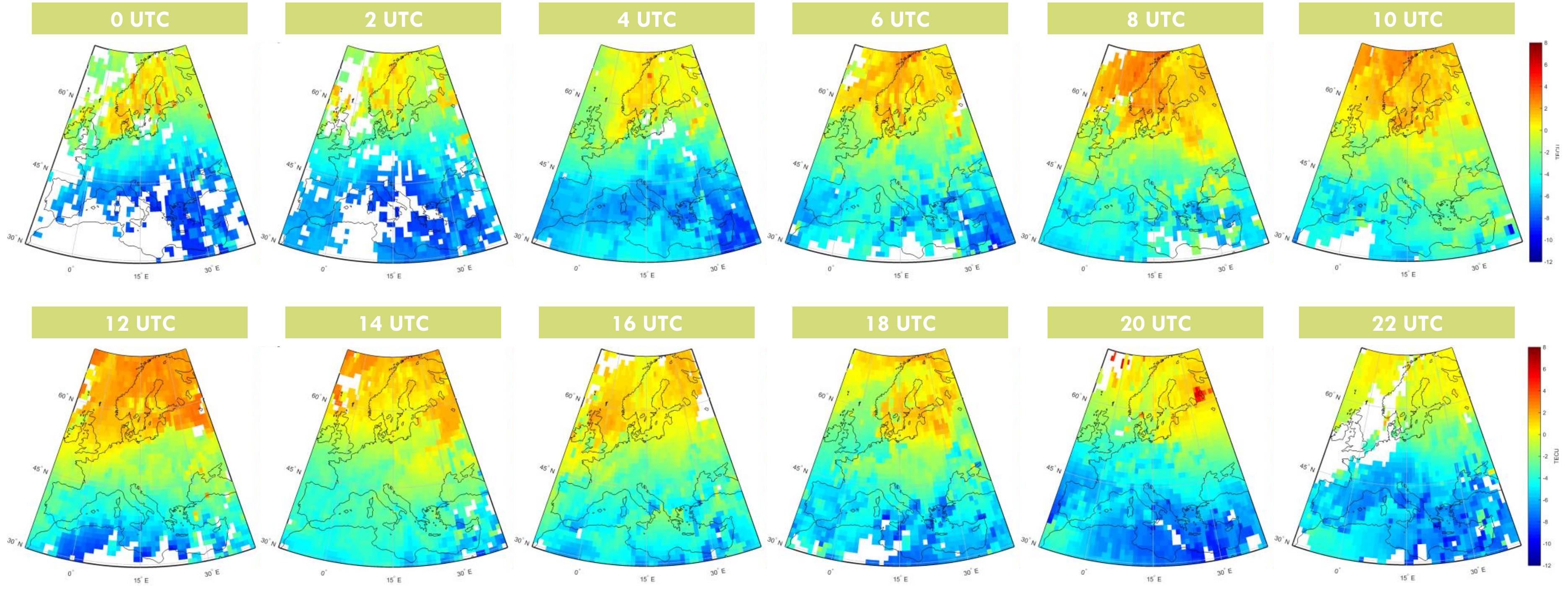

Differences: H2PT – NeQuick, grid: 1°; March 10, 2019

(scale: -12 ÷ 8 TECU)

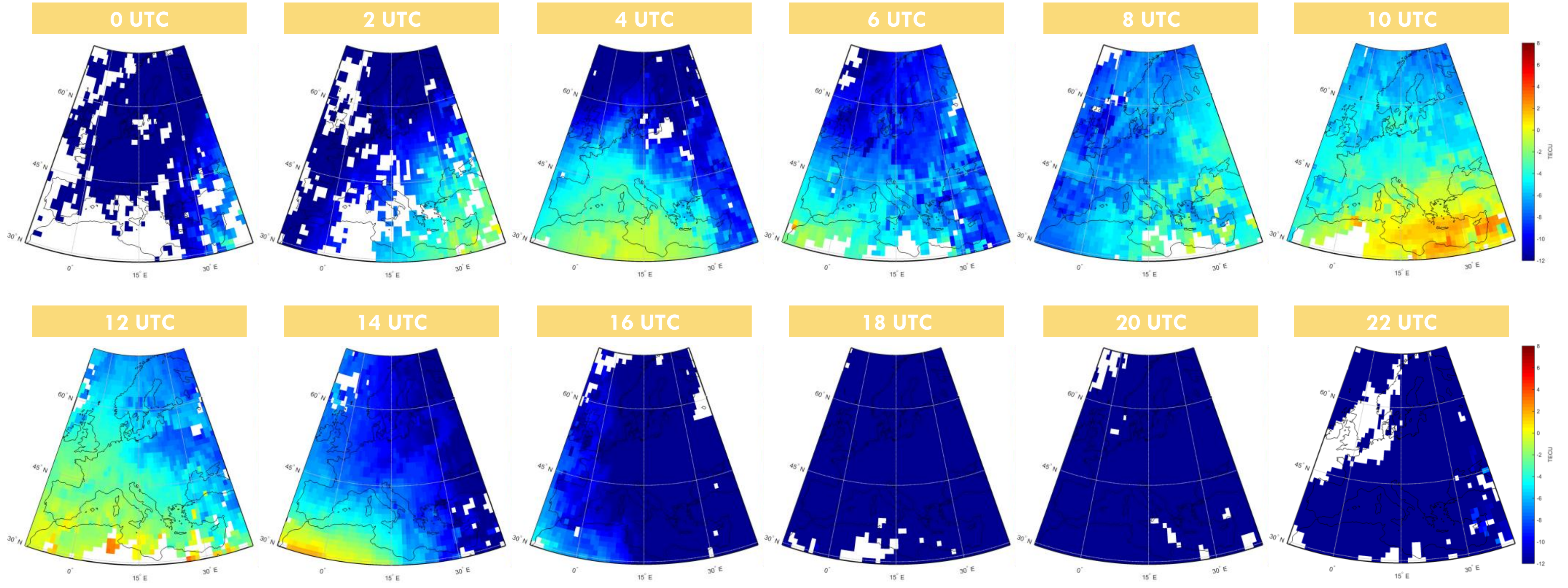

Statistical parameters, grid: 1°, March 10, 2019

2 UTC	min [TECU]	max [TECU]	amplitude [TECU]	mean [TECU]	σ [TECU]	correlation coefficient [-]
H2PT	0,2	5,9	5,7	1,15	0,94	
IGS	1,4	8,9	7,5	5,02	2,71	
NeQuick	2,9	17,6	14,7	11,18	3,73	
$\Delta_{H2PT-IGS}$	-8,9	2,3	11,2	-3,63	3,00	-0,20
$\Delta_{H2PT-NeQuick}$	-17,0	0,3	17,3	-10,09	3,77	0,06

8 UTC	min [TECU]	max [TECU]	amplitude [TECU]	mean [TECU]	σ [TECU]	correlation coefficient [-]
H2PT	1,7	12,6	10,9	6,58	1,73	
IGS	3,2	14,9	11,7	7,97	3,25	
NeQuick	11,7	14,4	2,7	12,78	0,52	
$\Delta_{H2PT-IGS}$	-6,9	3,7	10,6	-1,27	2,65	0,51
$\Delta_{H2PT-NeQuick}$	-11,1	-0,2	10,9	-6,18	1,71	0,18

14 UTC	min [TECU]	max [TECU]	amplitude [TECU]	mean [TECU]	σ [TECU]	correlation coefficient [-]
H2PT	4,0	15,8	11,8	8,23	2,22	
IGS	3,9	19,8	15,9	9,55	4,07	
NeQuick	12,5	22,3	9,7	16,83	2,15	
$\Delta_{H2PT-IGS}$	-8,5	3,3	11,8	-1,35	2,28	0,90
$\Delta_{H2PT-NeQuick}$	-16,9	2,0	18,9	-8,60	3,13	-0,04

20 UTC	min [TECU]	max [TECU]	amplitude [TECU]	mean [TECU]	σ [TECU]	correlation coefficient [-]
H2PT	0,5	7,9	7,4	2,53	1,30	
IGS	1,3	10,5	9,2	5,61	3,19	
NeQuick	18,8	24,5	5,7	21,44	1,32	
$\Delta_{H2PT-IGS}$	-9,2	6,0	15,2	-3,13	3,06	0,29
$\Delta_{H2PT-NeQuick}$	-24,1	-12,0	12,1	-18,93	1,91	-0,05

Time series, $\lambda = 20°E$, date: January 15, 2019

H2PT (scale: 0 ÷ 20 TECU)

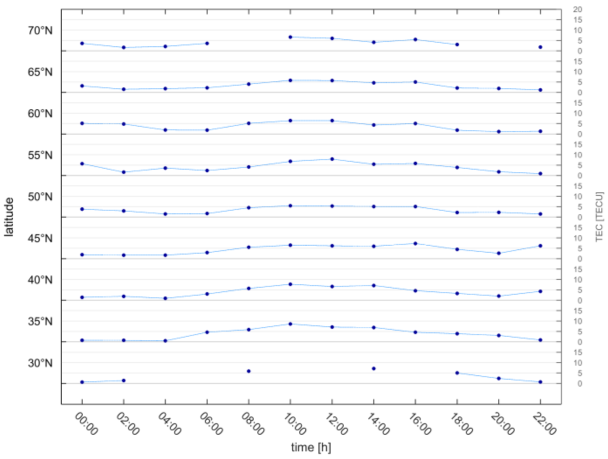

IGS (scale: 0 ÷ 20 TECU)

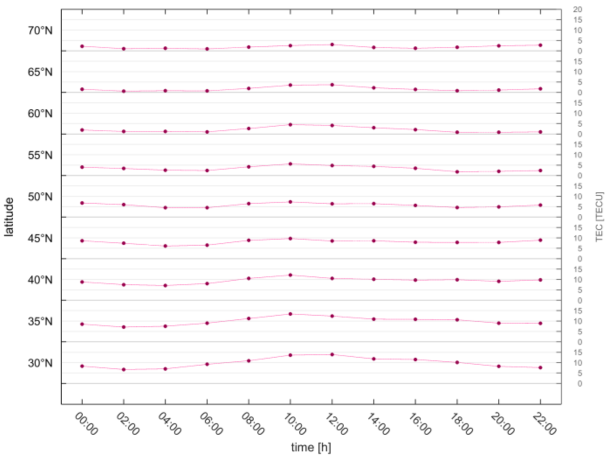

differences (scale: -12 ÷ 8 TECU)

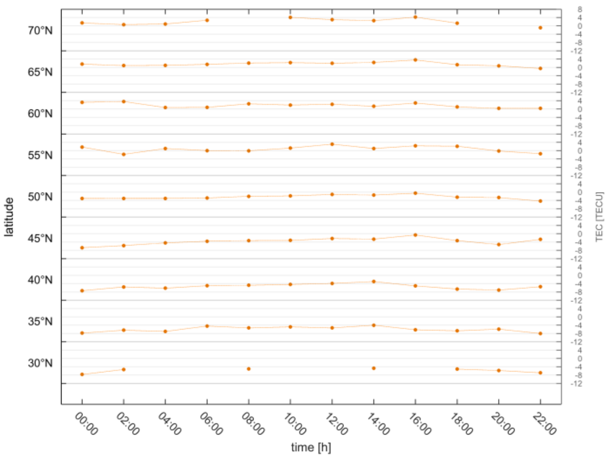

Time series, $\lambda = 20°E$, date: February 21, 2019

H2PT (scale: 0 ÷ 20 TECU)

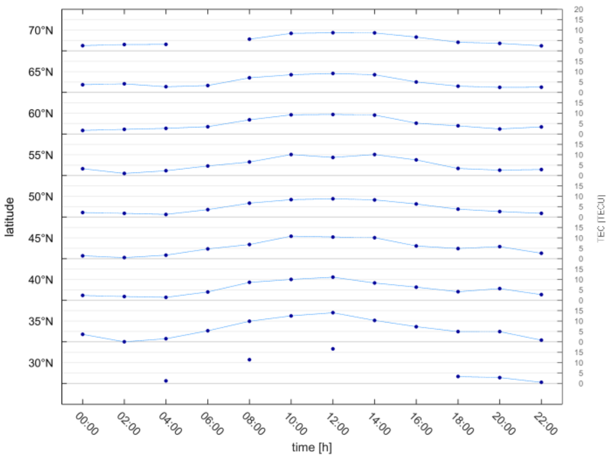

IGS (scale: 0 ÷ 20 TECU)

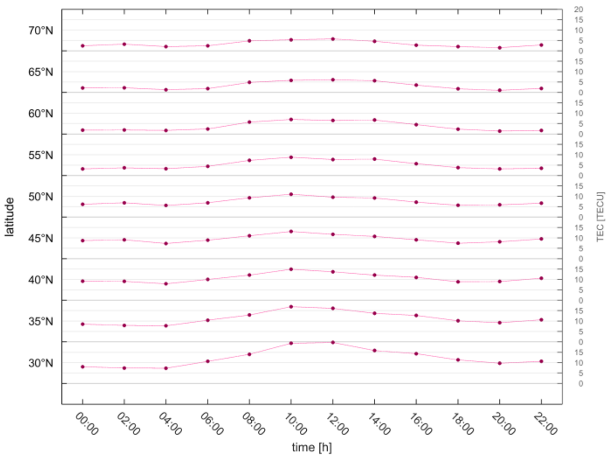

differences (scale: -12 ÷ 8 TECU)

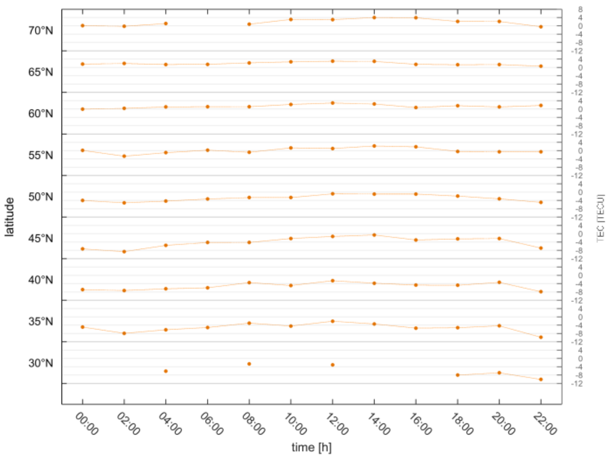

Time series, $\lambda = 20°E$, date: March 10, 2019

H2PT (scale: 0 ÷ 20 TECU)	IGS (scale: 0 ÷ 20 TECU)	**differences** (scale: -12 ÷ 8 TECU)

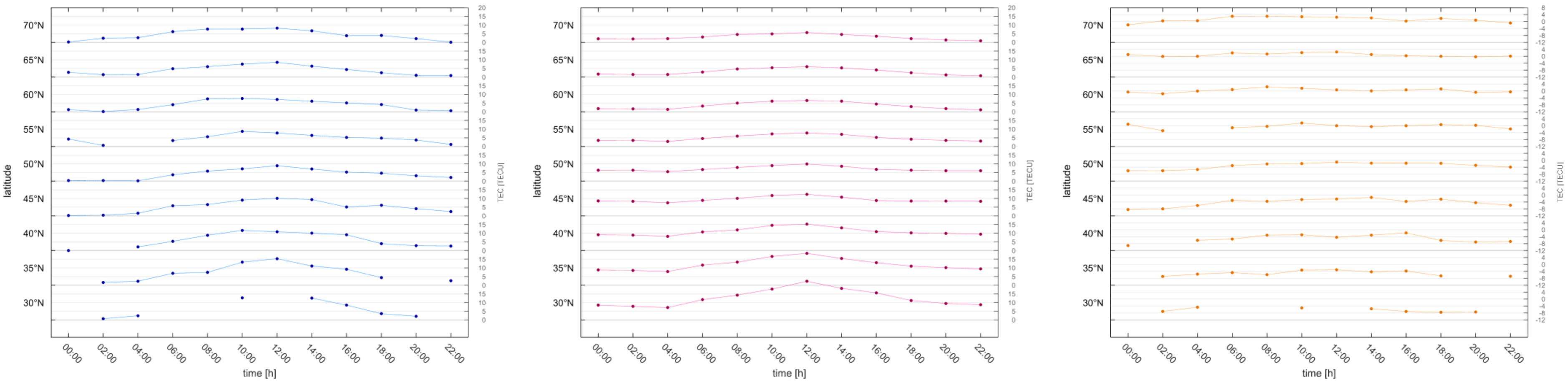

Conclusions – TEC parameter

- the presented maps, tables and plots are in line with the general trend that can be seen by comparing the H2PT, IGS and NeQuick-G models

- **H2PT vs IGS**
  - differences in TEC parameter values occur in particular depending on latitude
  - in the case of the high latitude regions, the values of the H2PT model are higher than the IGS model (overestimated), while in the middle latitude areas – inversely (underestimated)
  - a higher correlation coefficient is recorded in the daytime
  - no constant relationship was observed in the correlation of models along a given parallel

- **H2PT vs NeQuick-G**
  - the TEC parameter in the NeQuick-G model is consistently much higher than in the H2PT model, regardless of location and time
  - mean differences range from several TECU during the day to about 20 TECU at night
  - the correlation coefficient is close to zero

- **H2PT 5° vs 1° grid**
  - 5° x 5° maps allow for preview, overall analyzes
  - 1° x1° maps give the opoortunity to carry out detailed interpretations, especially in the context of ionospheric disturbances

Analysis

hmF2 parameter

TEC & hmF2 maps, December 28, 2018 (positively disturbed)

(scale: 0 ÷ 20 TECU and 150 ÷ 350 km, accordingly)

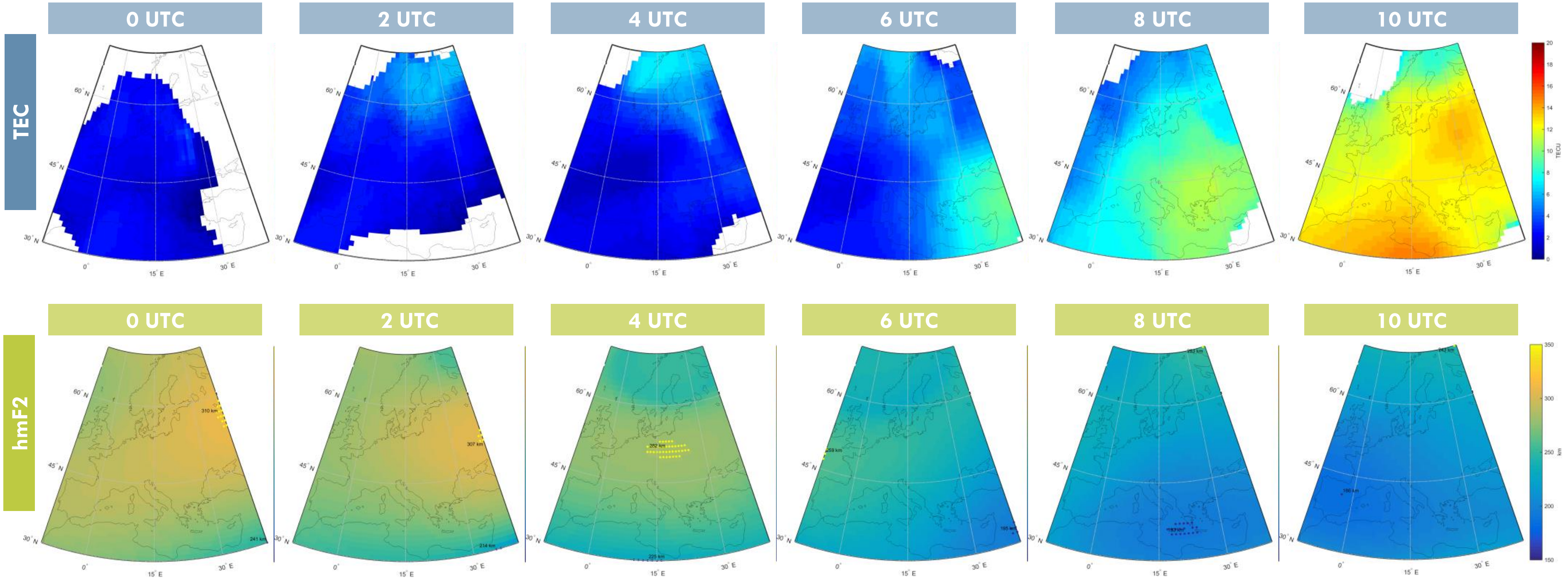

TEC & hmF2 maps, December 28, 2018 (positively disturbed)

(scale: 0 ÷ 20 TECU and 150 ÷ 350 km, accordingly)

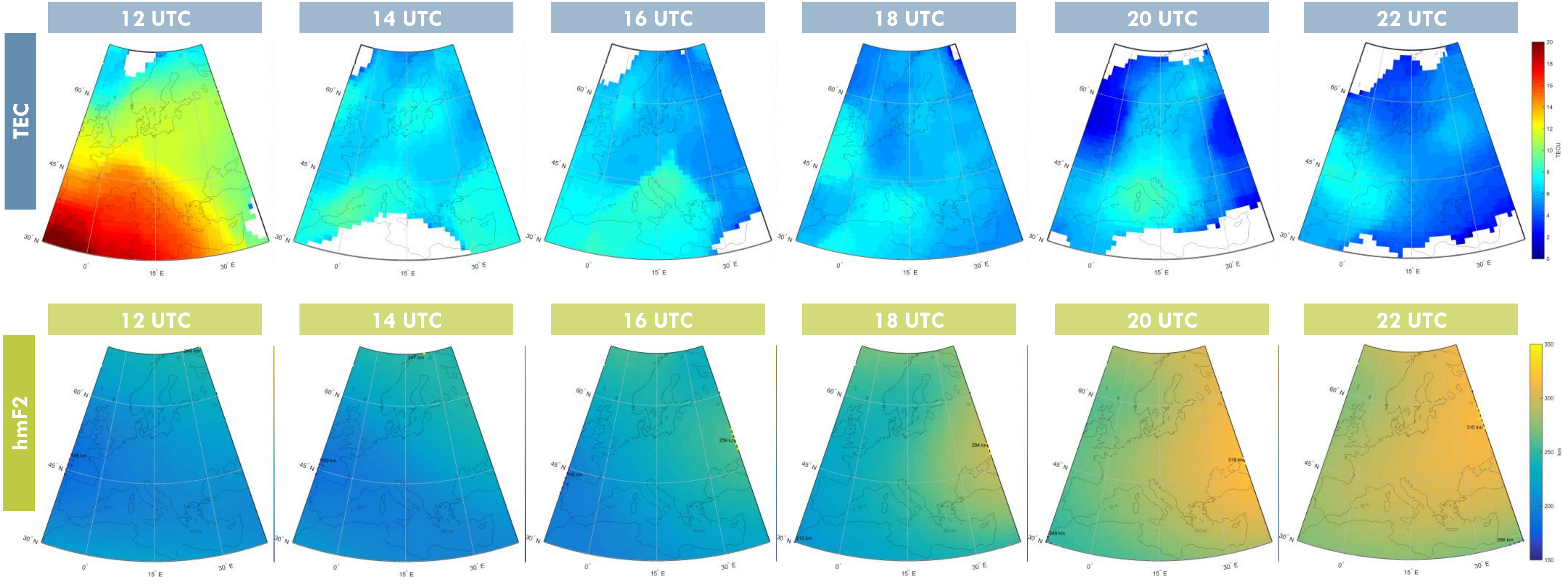

Statistical parameters, December 28, 2018 (positively disturbed)

TEC parameter					
UTC	min [TECU]	max [TECU]	amplitude [TECU]	mean [TECU]	σ [TECU]
0	0,2	4,2	4,0	1,99	0,56
2	0,4	4,2	3,8	1,99	0,56
4	1,0	7,1	6,1	3,18	1,72
6	1,7	9,6	7,9	4,72	1,85
8	3,5	11,1	7,6	7,65	1,83
10	6,6	15,1	8,5	12,07	1,43
12	3,9	20,8	16,9	12,10	3,21
14	3,8	9,3	5,5	6,91	0,79
16	3,4	8,7	5,3	6,40	1,06
18	1,3	7,9	6,6	6,04	0,75
20	0,9	8,7	7,8	5,49	1,65
22	0,2	7,9	7,7	5,12	1,14

hmF2 parameter					
UTC	min [km]	max [km]	amplitude [km]	mean [km]	σ [km]
0	241	310	69	288,6	11,9
2	214	307	93	279,1	15,7
4	225	282	57	262,2	14,2
6	195	259	64	235,3	13,9
8	193	253	60	217,4	15,4
10	186	243	57	210,3	14,4
12	186	244	58	212,9	13,1
14	190	247	57	217,6	17,3
16	196	259	63	230,1	16,5
18	212	294	82	251,7	18,5
20	249	318	69	284,8	16,7
22	266	315	49	294,1	11,7

TEC & hmF2 maps, December 31, 2018 (negatively disturbed)

(scale: 0 ÷ 20 TECU and 150 ÷ 350 km, accordingly)

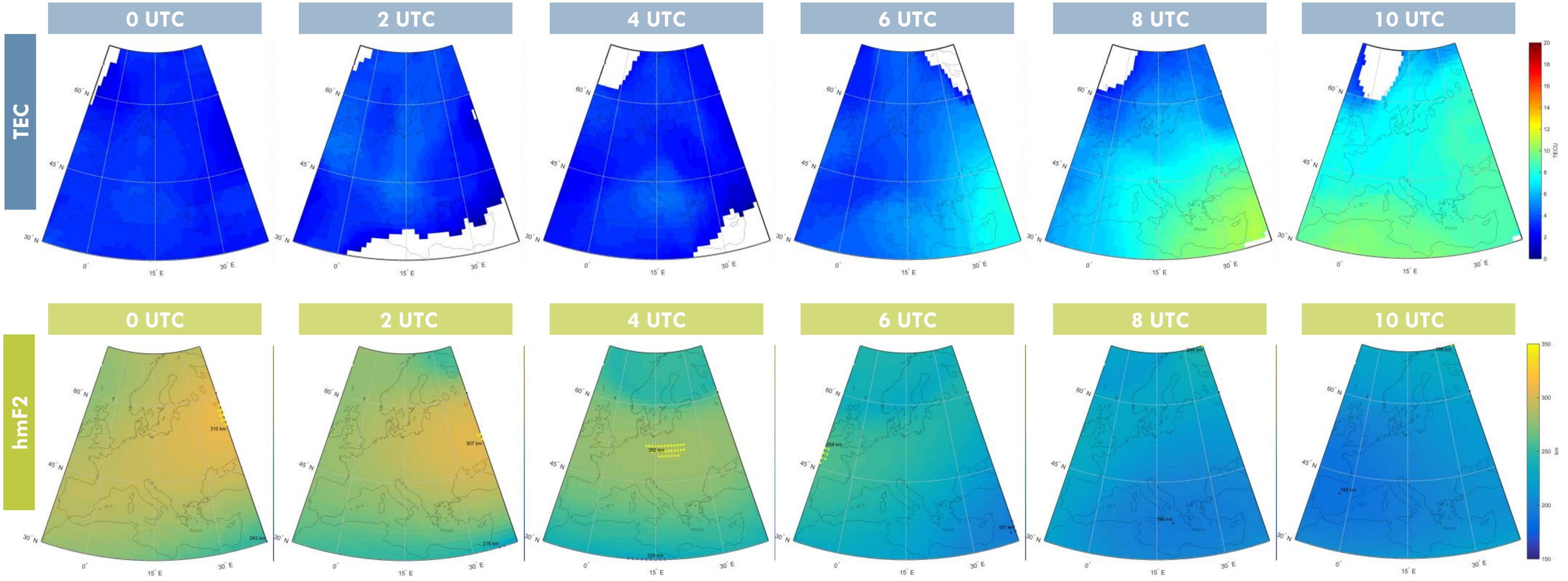

TEC & hmF2 maps, December 31, 2018 (negatively disturbed)

(scale: 0 ÷ 20 TECU and 150 ÷ 350 km, accordingly)

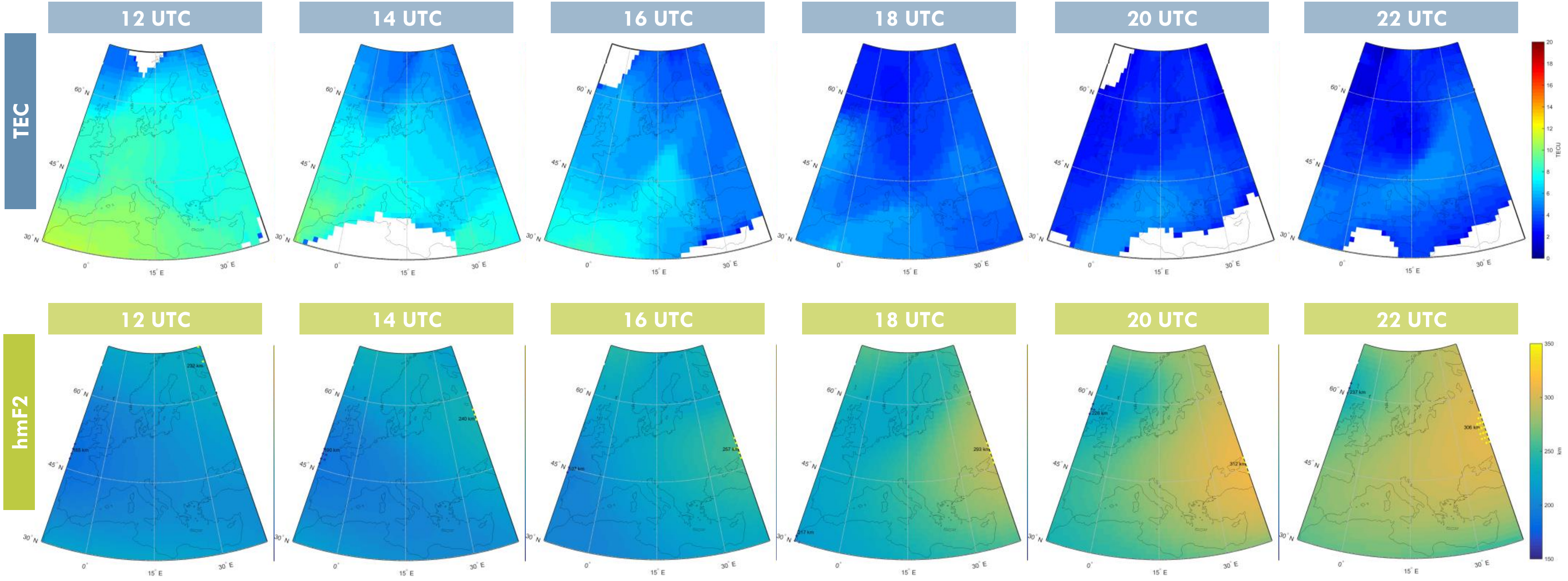

Statistical parameters, December 31, 2018 (negatively disturbed)

TEC parameter					
UTC	min [TECU]	max [TECU]	amplitude [TECU]	mean [TECU]	σ [TECU]
0	1,6	3,9	2,3	3,03	0,40
2	0,1	4,7	4,6	3,39	0,73
4	0,2	4,5	4,3	2,99	0,59
6	2,7	8,1	5,4	4,65	1,23
8	2,8	10,7	7,9	6,55	1,88
10	2,7	10,2	7,5	7,99	1,21
12	2,6	11,2	8,6	7,94	1,47
14	4,2	10,0	5,8	6,47	1,21
16	1,8	8,6	6,8	5,46	1,11
18	1,8	6,6	4,8	4,07	0,81
20	0,8	5,5	4,7	3,49	0,79
22	0,9	5,2	4,3	3,64	0,95

hmF2 parameter					
UTC	min [km]	max [km]	amplitude [km]	mean [km]	σ [km]
0	243	310	67	288,4	11,4
2	215	307	92	278,7	15,4
4	228	282	54	262,1	14,0
6	197	259	62	235,3	13,4
8	196	244	48	215,3	11,6
10	188	234	46	208,6	11,5
12	185	232	47	210,8	11,0
14	190	240	50	214,9	13,4
16	197	257	60	226,5	13,4
18	217	293	76	247,4	18,2
20	226	312	86	270,0	21,4
22	237	306	69	281,0	15,0

TEC & hmF2 maps, December 30, 2018 (quiet)

(scale: 0 ÷ 20 TECU and 150 ÷ 350 km, accordingly)

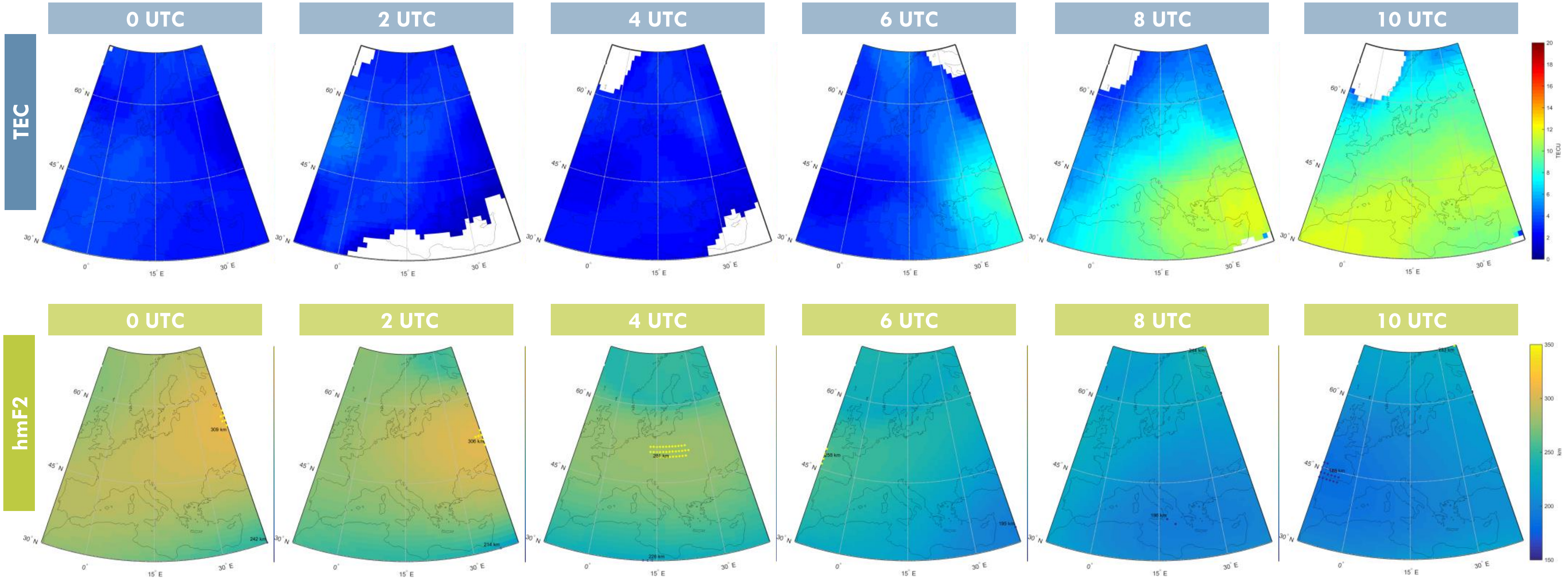

TEC & hmF2 maps, December 30, 2018 (quiet)

(scale: 0 ÷ 20 TECU and 150 ÷ 350 km, accordingly)

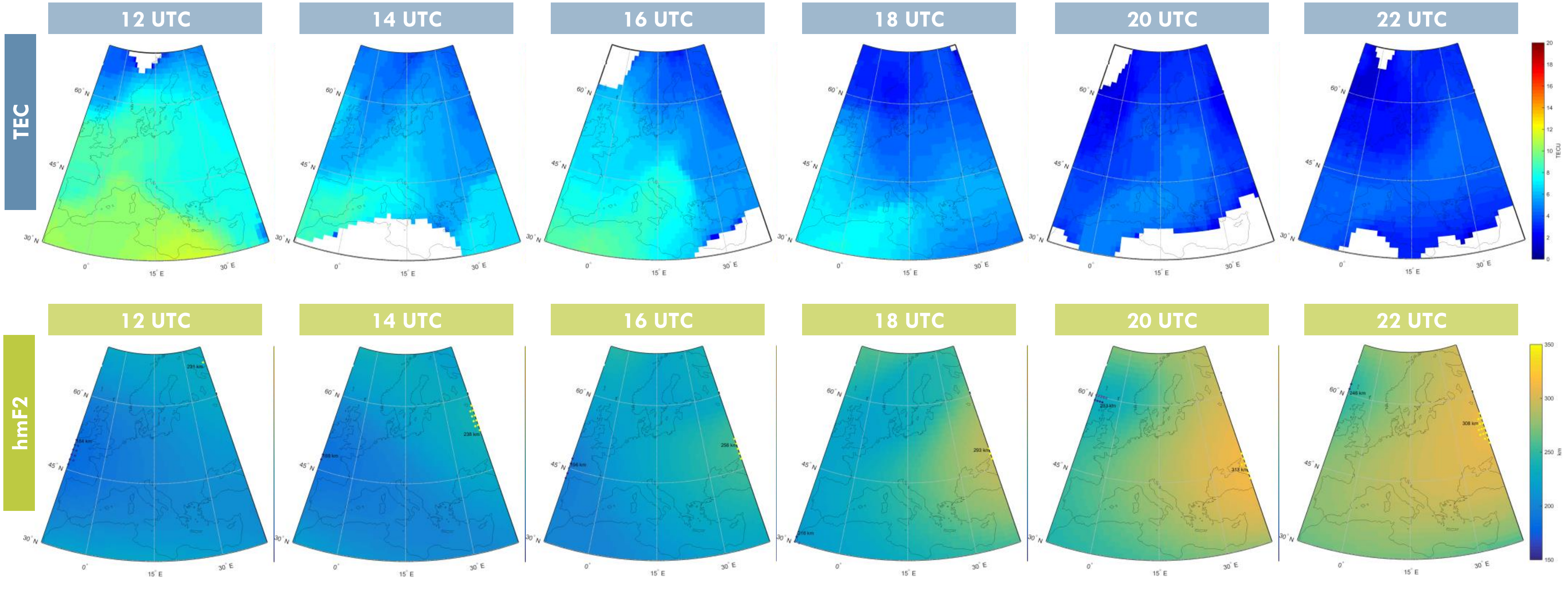

Statistical parameters, December 30, 2018 (quiet)

TEC parameter					
UTC	min [TECU]	max [TECU]	amplitude [TECU]	mean [TECU]	σ [TECU]
0	1,4	3,9	2,5	3,06	0,50
2	0,6	4,7	4,1	3,08	0,75
4	1,3	3,6	2,3	2,58	0,42
6	2,1	9,1	7,0	4,25	1,53
8	2,9	11,8	8,9	7,41	2,36
10	3,2	11,9	8,7	9,49	1,65
12	2,0	11,5	9,5	8,06	1,72
14	3,7	8,7	5,0	5,87	1,05
16	2,2	9,5	7,3	6,09	1,48
18	1,2	7,9	6,7	4,92	1,29
20	1,1	5,1	4,0	3,64	0,79
22	0,6	4,5	3,9	3,43	0,76

hmF2 parameter					
UTC	min [km]	max [km]	amplitude [km]	mean [km]	σ [km]
0	242	309	67	286,9	11,4
2	214	306	92	277,0	15,6
4	226	281	55	260,8	14,0
6	195	258	63	234,0	13,3
8	196	244	48	214,9	11,7
10	186	233	47	207,5	11,5
12	184	231	47	209,7	11,2
14	188	238	50	213,6	13,4
16	196	256	60	225,2	13,3
18	216	293	77	246,0	18,5
20	233	313	80	273,9	19,9
22	246	308	62	284,5	13,6

Conclusions – hmF2 parameter

- hmF2 parameter varies greatly throughout the day
  - during the night may fall below 200 km above the Earth's surface
  - during the day can exceed 300 km
  - the difference to the usually defined value of 450 km remains significant
- the relationship between the time of day (and consequently the TEC parameter value) and the height of hmF2 can be clearly seen
  - if the TEC parameter increases, hmF2 falls closer to the Earth
  - if the TEC parameter is low, hmF2 climbs higher

Analysis

Disturbed conditions – examples

Time series – distrubed days and median for the whole day

January, 2019

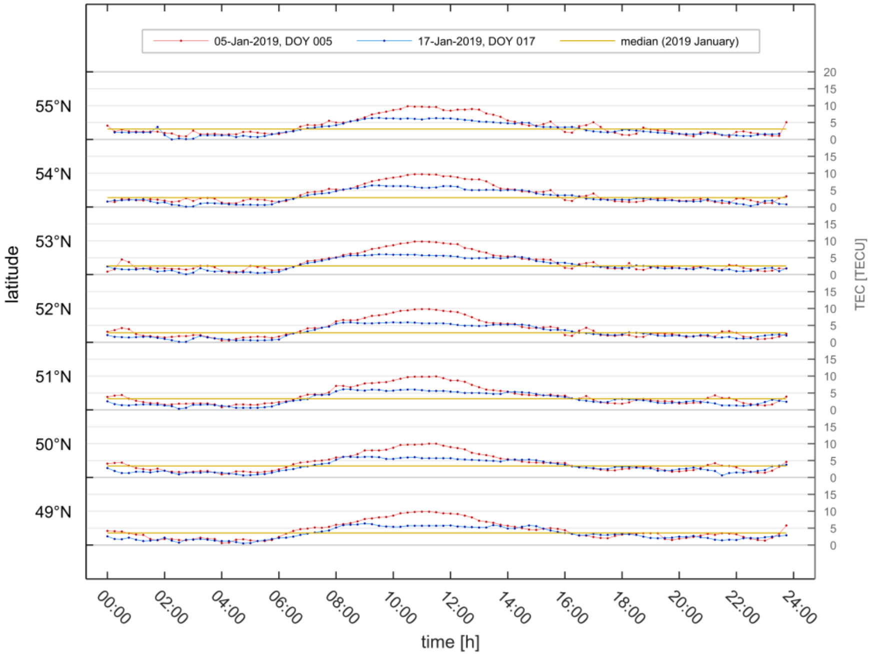

February, 2019

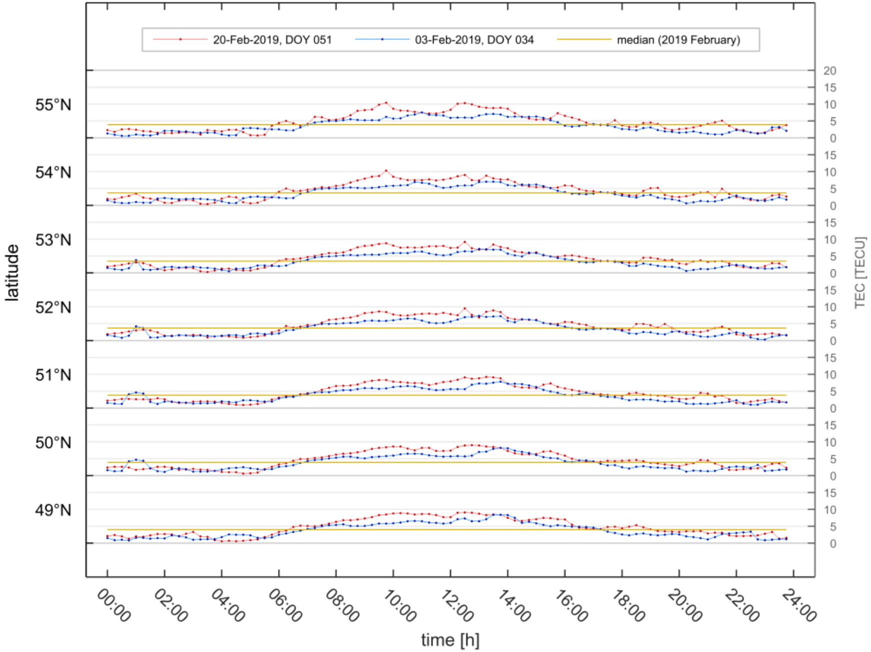

Time series – distrubed days and median for subsequent hours

January, 2019

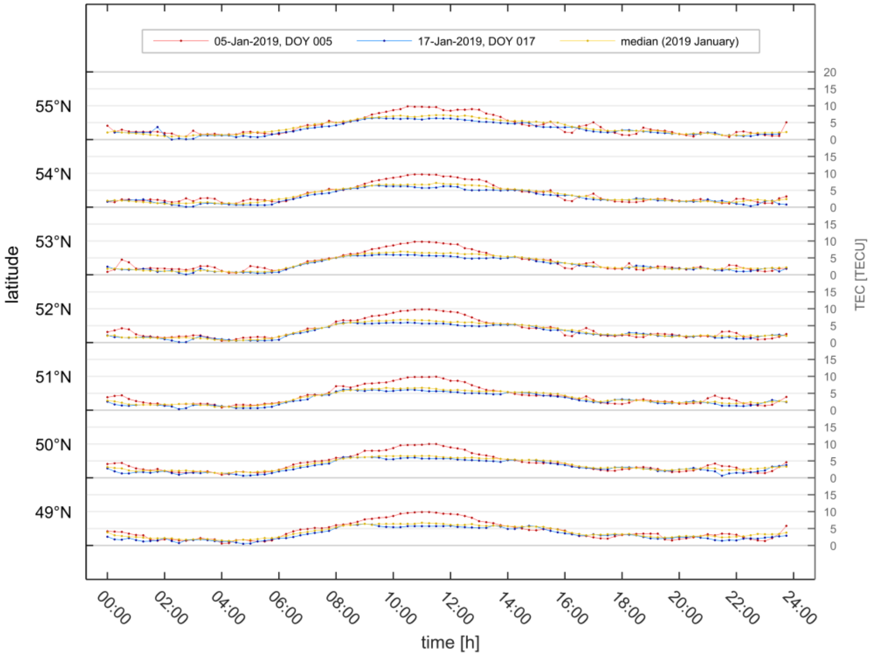

February, 2019

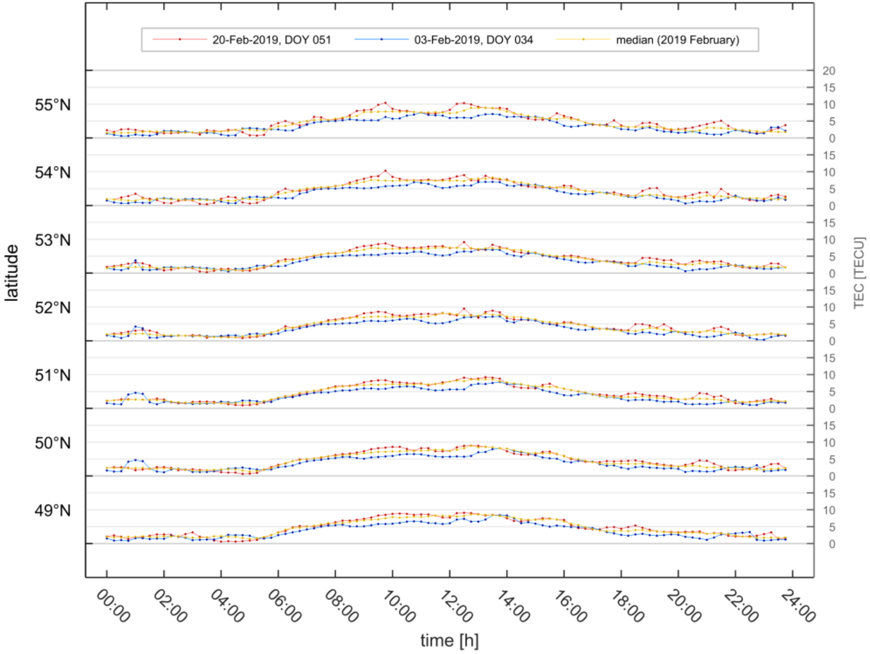

Time series – distrubed and quiet days

January, 2019

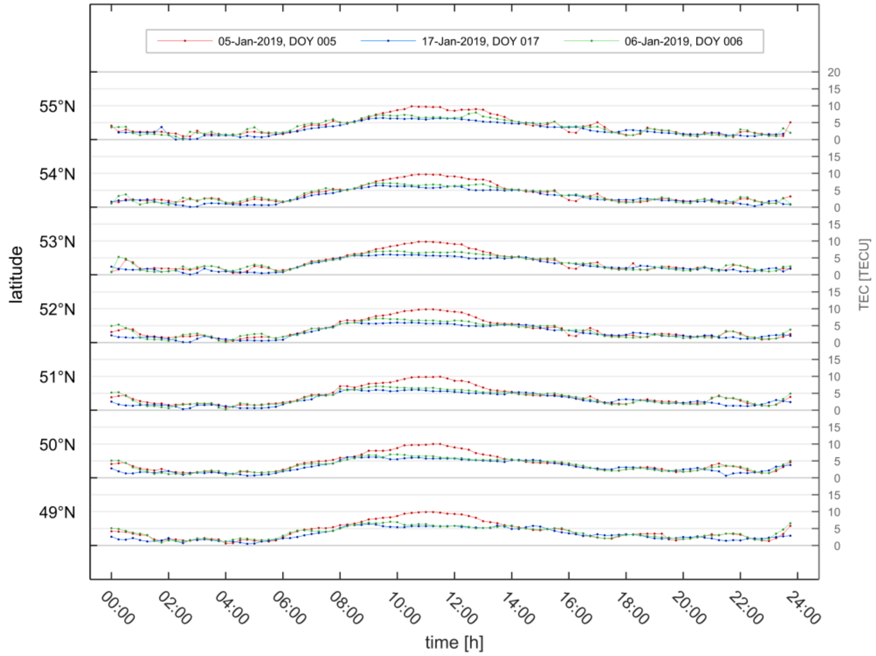

February, 2019

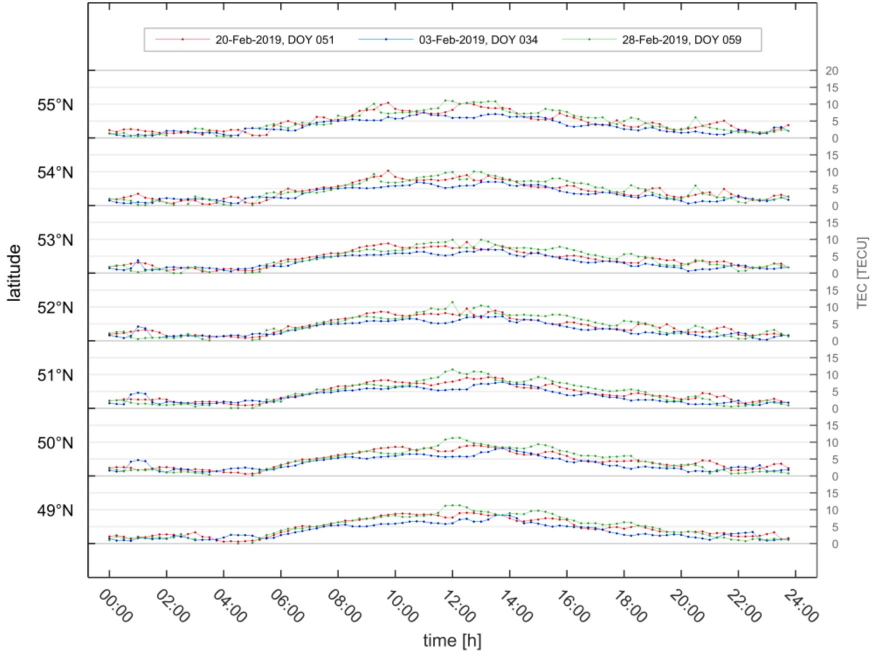

Conclusions – disturbed conditions

- the plots present the H2PT model data with a time resolution of 15 minutes and a spatial resolution of 1° x 1° for the location of Warsaw (latitude: 52°N, longitude: 21°E)
- positive and negative disturbances were considered based on the confrontation with:
  - median for the entire month (common value for the whole day)
  - median for individual hours over all days of the month (with a 15-minute interval)
  - quiet day
- solutions usability:
  - the first option (median for the whole day) causes a large data degradation because it eliminates the typical variability of ionosphere activity in the daily course
  - in the case of the third solution, quiet day term is relative and uncertain
  - the most reliable approach represents the second option – median for subsequent hours
- high time resolution allows to indicate occuring ionosphere condition disturbances, both positive and negative

Summary

Conclusions

- the H2PT model is of the regional type, is dedicated to the Europe area, which allows focusing on a relatively small territory, but with greater accuracy
- resolution is an undoubted advantage of the model; maps are generated for 15 minutes epochs, while the grid (in a more accurate version) has dimensions 1° x 1°
- high temporal resolution allows detection of disturbances that last only a few hours, and therefore cannot be accurately detected on the base of 2 hour interval data
- high spatial resolution enables detailed analysis of occuring ionosphere disturbances
- the course of the TEC parameter for the days during which a positive or negative disturbance occurred gives a reliable overview in comparison with the median computed for each epoch during the day independently
- as the ionosphere layers height varies dependently on the latitude, for Europe area the location of hmF2 significantly differs from the value adopted for the entire globe, amounting to 450 km
- if the appropriate height of hmF2 in a given time and location is taken into account when processing GNSS data and estimating ionospheric correction, it may positively affect the positioning quality

Contact

Co-author	E-mail
Paulina Woźniak	pwozniak@cbk.waw.pl
Anna Świątek	ana@cbk.waw.pl
Mariusz Pożoga	pozoga@cbk.waw.pl
Łukasz Tomasik	tomasik@cbk.waw.pl

Space Research Centre

Polish Aacademy of Sciences

Warsaw, Poland

Paulina Woźniak
Anna Świątek
Mariusz Pożoga
Łukasz Tomasik

Space Research Centre
Polish Aacademy of Sciences
Warsaw, Poland

Analysis of a new regional ionospheric assimilated **H2PT model** for Europe

European Geosciences Union General Assembly
3-8 May 2020, Vienna, Austria